Journal of Polymer Science and Engineering (2023) Volume 6 Issue 1
doi: 10.24294/jpse.v6i1.2405

ORIGINAL RESEARCH ARTICLE

Silver-based plasmonic nanoparticles and their application as biosensor

Pratima Parashar Pandey

School of Science & Engineering, IILM University, Greater Noida 201306, India; pratimaparashara@rediffmail.com

ABSTRACT

The silver nanoparticles (AgNPs) exhibit unique and tunable plasmonic properties. The size and shape of these particles can manipulate their localized surface plasmon resonance (LSPR) property and their response to the local environment. The LSPR property of nanoparticles is exploited by their optical, chemical, and biological sensing. This is an interdisciplinary area that involves chemistry, biology, and materials science. In this paper, a polymer system is used with the optimization technique of blending two polymers. The two polymer composites polystyrene/poly (4-vinylpyridine) (PS/P4VP) (50:50) and (75:25) were used as found suitable by their previous morphological studies. The results of 50, 95, and 50, 150 nm thicknesses of silver nanoparticles deposited on PS/P4VP (50:50) and (75:25) were explored to observe their optical sensitivity. The nature of the polymer composite embedded with silver nanoparticles affects the size of the nanoparticle and its distribution in the matrix. The polymer composites used are found to have a uniform distribution of nanoparticles of various sizes. The optical properties of Ag nanoparticles embedded in suitable polymer composites for the development of the latest plasmonic applications, owing to their unique properties, were explored. The sensing capability of a particular polymer composite is found to depend on the size of the nanoparticle embedded in it. The optimum result has been found for silver nanoparticles of 150 nm thickness deposited on PS/P4VP (75:25).

Keywords: silver nanoparticles; polymer composite; thin films; vapor deposition; biosensors

ARTICLE INFO

Received: 14 July 2023
Accepted: 4 August 2023
Available online: 13 September 2023

1. Introduction

Silver nanocomposites have been of enormous interest due to their commercial applications in medical, electronic, chemical, and biochemical sensors and devices. Nanocomposites are multiphase materials where at least one of the phases has a dimension on the nano-scale. These new nanomaterials have applications in novel, highly sensitive analytical devices[1]. The new development in nanotechnology is biosensor-based nanomaterials. These materials have made a made a great contribution to the improvement of the sensitivity of biomolecular detection. Nanobiomaterials represent the integration of material science, molecular engineering, chemistry, and biotechnology. The nanomaterial sensors are capable of manipulating atoms and molecules for their application as detection devices. The biosensor-based nanomaterial composite has great potential in applications such as biomolecule recognition, pathogenic diagnosis, and environmental monitoring[2–4].

The polymer composites are used as a base for preparing nanobiomaterials where silver nanoparticles are embedded into polymer matrices. The polymer is used as a particle stabilizer to prevent the agglomeration of these particles. In the recent past, silver

nanoparticles embedded in polymer composites have been very desirable owing to the applications of silver nanocomposites in various fields such as catalysis, drug delivery, wound dressing, antimicrobial activity, sensors, and optical information storage. It is well known that small silver particles embedded in polymer matrix exhibit plasmon resonance absorption, and as a result, absorption maxima occur in the visible-near infrared region, and their spectral position depends on the particle size, shape, filling factor, etc., in the polymer matrix. The surface plasmon resonance absorption for silver clusters in the polymer matrix generally occurs at a wavelength of ~430 nm. The shift in the plasmon resonance peak towards a higher wavelength occurs due to the close proximity of the silver clusters. These nanoparticles exhibit unique optical properties originating from the characteristic surface plasmon formed by the collective motion of conduction electrons. The spectral position, half width, and intensity of the plasmon resonance strongly depend on the particle size, shape, and dielectric properties of the particle material and the surrounding medium. Thus, the type of metal and the surrounding dielectric medium play a significant role in the excitation of particle plasmon resonance (PPR). The sensitivity of PPR frequency to small variations of these parameters can be exploited in various applications. The differing natures of the polymeric hosts yield changes in dispersion, size distribution, and impregnation depth of silver clusters.

The high conductivity and high thermal stability of silver make it an important and favorite metal among all the metals to produce nanoparticles. Also, it is one of the most important materials in plasmonics[5]. AgNPs are of great importance due to their unique electrical, thermal, catalytic, optical, and sensing characteristics. All these properties are suitable for applications in biomolecule detection, immunoassays, surface plasmon optics, data storage, catalysis, surface-enhanced Raman scattering, antibacterial material, photonics, and photography[6]. But AgNPs have been found to be unstable and agglomerate in aqueous media. This problem can be overcome by immersing them in polymer matrices[7–10]. Apart from this, AgNPs have been found to be toxic in human cells and the ecological system; therefore, encapsulating them in polymer matrices reduces their adverse effects. Embedding AgNPs in various polymer matrices enhances their thermal, optical, mechanical, and conducting properties so that they become useful for application in many optical and sensing devices[11]. Therefore, two compositions of polymer composites are analyzed here as their applications in the sensors. The size of silver clusters in a particular composite is manipulated by the different thicknesses of silver deposited on them, yielding different sizes of nanoparticles.

The synthesis of silver nanoparticles by ex situ methods does not provide homogeneous dispersion into the host polymer composite due to their easy agglomeration. Now, preparing silver nanoparticles of various shapes and sizes in different polymer matrices is possible by different methods. The toxic and potentially hazardous reactants are used in many ways, causing environmental disorder. Therefore, using eco-friendly methods is the need of the hour.

The vacuum evaporation of metal onto softened polymer composites forms island or discontinuous metal films by stopping the deposition at a very early stage. This is the simplest and most eco-friendly technique to prepare silver nanoparticles. However, such structures face temporal instability even in a vacuum, possibly due to the mobility of islands followed by coalescence[12]. Also, when these films are exposed to the atmosphere, they get oxidized. As a result, an irreversible increase in electrical resistance is found due to the oxidation of islands of nanoparticles[13]. Various inorganic materials deposited on softened polymer composites are reported in the literature[14–17]. The surface morphology of subsurface discontinuous metal films depends on thermodynamic as well as deposition parameters[16,17]. The polymer substrats are softened in order to keep control of the viscosity of the substrate so that the silver nanoparticles can be embedded into polymer composites. The polymer-metal interaction influences the morphology of silver nanoparticles that form inside polymer matrices[10,18,19]. The samples used for this study were prepared by vacuum evaporation of silver on

polymer composites at high temperatures of 10^{-6} Torr. A wide range of applications can be created by precise tailoring and optimization of the nanocomposite structures.

Blending is the process of combining the properties of polymers in order to achieve a desirable polymer system. In the present system of polymers, the property of polystyrene (PS) is combined with poly (4-vinyl pyridine) (P4VP). The stability of PS is combined with P4VP in order to achieve a small size and uniform distribution of silver in the PS/P4VP composite. Among the various compositions of polymers, a suitable polymer composite is explored. The silver nanoparticles embedded into PS/P4VP (50:50, 75:25) have shown room temperature resistances in the range of a few tens to a few hundred MΩ/per sheet, which is desirable for device applications.

Applications of AgNPs for biosensors have been found rarely in the literature as compared to gold nanoparticles (AuNPs). The studies on AgNP plasmonic biosensors have found even less. Though most of the sensors operate ex vivo, the toxicity of AgNPs is a major concern. The other limitation of using these particles as bares for biosensing is due to their poor stability and unusual surface chemistry[20,21]. To avoid such constraints, coatings of AgNPs were done in order to overcome the stability and toxicity of AgNPs in a given environment with a large variety of compounds[22,23]. Also, the aggregation of NPs can be overcome by coating the NPs, which provides electrostatic, steric, or electrosteric repulsive forces between the particles[20]. The various coating methods that have been found in the literature for covering AgNPs with an organic or inorganic medium for plasmonic biosensing applications. Embedment of silver into polymer matrices is a successful method where silver nanoparticles are dispersed uniformly in polymer composites, restricting the agglomeration of nanoparticles. A decisive influence on the optical properties of the NPs depends on the nature of the coating material and its thickness. The unique feature of this hybrid quanta system is exploited in plasmonic systems and devices. The optical sensors are used for refractive index measurement in the biomedical, chemical, and food processing industries. Thus, materials scientists are keenly focused on the exploration of ultrasensitive plasmonic detectors for biosensing applications[24,25]. The present study is about the plasmonic biosensing response of AgNPs embedded in polymer composites in order to improve electrostatic, steric, and electrosteric stabilization of AgNPs.

2. Experimental

The polymers used in this study are of laboratory grade, detail report is given in previous paper[9]. The structure of P4VP and PS are (a) and (b), respectively, as follows:

(a) (b)

The various polymer compositions are prepared as described in our previous report[9]. Further, the deposition of silver onto desirable polymer systems, PS/P4VP (50:50) and (75:25), is carried out as described in the paper of Parashar[9].

In this paper, the optical properties of the best samples claimed in our previous results[8], i.e., PS/P4VP (50:50) for 50 and 95 nm and PS/P4VP (75:25) for 50 and 150 nm, were used, and their sensor responses were recorded using nanosensor lab software. This computational tool is based on mie theory for investigating the

optical response of low-dimensional structures for core-shell nanoparticles and nanomatryoshka and the extinction efficiencies, scattering efficiencies, and absorption efficiencies. This tool is designed for refractive index sensors to simulate sensitivity, figure of merit, quality factor, FWHM (full width at half maximum frequency), and scattering of electromagnetic radiation by coreshell spherical nanoparticles. It has been designed as a virtual laboratory, including a friendly graphical user interface (GUI), an optimization algorithm (to fit the simulations to experimental results), and scripting capabilities. As per our previous results of morphological studies of silver nanoparticles embedded in the above polymer composites, the size of the nanoparticles is almost spherical. Therefore, design considerations for a spherical nanoparticle-based simulator panel are used. We have calculated the scattering, absorption, and extension efficiency by using a flow chart and entering the parameters as follows:

- In the geometrical panel, the average size of the nanopartcle is taken from the previous study on morphology[9], e.g., for the thickness of 50 nm for silver on PS/P4VP (50:50), R1 = 80 nm.
- The wavelength range is selected between min 400 nm, max 1200 nm, and steps 1000.
- In the material section, import Ag data and plot.
- The sensing parameter is selected as 'n = 1.33'.
- In the study section, a compute command is given.
- Calculated results are displayed as graphs.

3. Result and discussion

Humidity sensors based on silver nanoparticles encapsulated in polymer composites have been mentioned in the past[25,26]. An organic/inorganic nanocomposites of poly (diphenylamine sulfonic acid) (PSDA), 3 mercaptopropyl trimethoxy silane (MPTMS), and nano-ZnO is prepared to make thin film humidity sensors. The humidity-sensing properties of the sensors were examined by impedance measurements in the range of 100 Hz–1 kHz. The sensitivity of samples increases by threefold as the value of impedance changes, along with good repeatability and stability in the range of 12% to 95% RH[25].

Another method reported about Ag/polymer nanocomposite synthesized by a chemical reduction process. The sensing properties are investigated by forming coatings on platinum interdigital electrodes. The sensor gives a reversible, selective, and rapid response that is proportional to levels of humidity within the range of 10% RH to 60% RH[26].

Polymer composites, either grafted or adsorbed with NPs, promote uniform dispersion of the NPs when embedded in the polymer matrix. The loading of silver on the polymer composite of the requisite composition could evolve into good optical sensors. Our previous study on the morphology of AgNPs embedded into polymer composites, PS/P4VP (50:50) and PS/P4VP (75:25), claimed the homogenous dispersion of silver nanoparticles for thicknesses of 50, 95, and 50, 150 nm, respectively[9]. The nature of the polymer system and the amount of silver deposited on them have been found to be effective in determining the size distribution and dispersion of silver nanoparticles[9]. It has been found that the embedment of AgNPs in the polymer composite enhances their properties[10,11]. Thus, a platform is formed for their applications in sensors due to their large surface area and small dimensions. A number of nanocomposites with various amounts of AgNPs could be explored for the fabrication of sensors and biosensors with an efficient nanopolymer composite[5].

The following mechanism explores sensing in silver nanocomposites to enable the fabrication and commercialization of highly selective and specific agents. The influence of AgNP on parameters such as shape and composition on the sensitivity and selectivity of the sensor is explored. The extinction efficiencies, scattering efficiencies, and absorption efficiencies are written below.

x is the size parameter, and the coefficients for scattered fields are defined as[27],

$$Qext = \frac{2}{x^2}\sum_{l=1}^{\infty}[2l+1]Re(a_1 + b_1) \quad (1)$$

$$Qsca = \frac{2}{x^2}\sum_{l=1}^{\infty}[2l+1](|a_1|^2 + |b_1|^2) \quad (2)$$

$$Qabs = Qext - Qsca \quad (3)$$

a_n and b_n are defined as follows,

$$a_n = \frac{\Psi_n(x_3)\, H_n^a(\mu_3 x_3) - \mu_3 Z_n^{(1)}(x_3)}{\xi_n(x_3) H_n^a(\mu_3 x_3) - \mu_3 Z_n^{(3)}(x_3)} \quad (4)$$

$$b_n = \frac{\Psi_n(x_3)\, H_n^b(\mu_3 x_3) - Z_n^{(1)}(x_3)}{\xi_n(x_3) H_n^b(\mu_3 x_3) - Z_n^{(3)}(x_3)} \quad (5)$$

where μ_1 and μ_2 are the refractive indices of the core and the shell, and $\mu_3 = (\mathcal{E}_3/\mathcal{E}_4)$ is the relative refractive index of the outer shell medium relative to the surrounding medium. Also, $x_1 = kR_1$, $x_2 = kR_2$ and $x_3 = kR_3$ are size parameters, and the Riccati-Bessel functions $\Psi_n(x) = x\,jn(x)$, $\chi n(x) = -xyn(x)$, $\xi_n(x) = xh(1)(x)$ of first kind and the logarithmic derivative of Ricatti-Bessel functions like $Z_n^{(1)}$, $Z_n^{(2)}$, $Z_n^{(3)}$ are written as $Z_n^{(1)} = \Psi'(x)/\Psi n(x)$, $Z_n^{(2)} = \chi'(x)/\chi_n(x)$ and $H^a{}_n(\mu_3 x_3)$, $H^b{}_n(\mu_3 x_3)$.

The most relevant sensing parameters are:

1) Quality factor (*QF*) of scattering resonance peak.
2) Sensitivity (*S*) and
3) Figure of merit (*FOM*).

The quality factor of resonant peak is defined as the ratio of resonant wavelength of peak to the full width at half maximum (FWHM) of the resonant peak as[28]

$$QF = \lambda_R/FWHM \quad (6)$$

This suggests that the resonant peak with a smaller FWHM corresponds to the higher quality factor. The sensitivity (*S*) of the sensor is defined as the rate of shift of the resonant peak wavelength λ_R with the variation in the refractive index (*n*) of the surrounding medium, and the same is mathematically written as

$$S = d\lambda_R/dn \quad (7)$$

The figure of merit (*FOM*) of the sensor is directly proportional to the quality factor of the resonant peak and the sensitivity, and the same is expressed as

$$FOM = \lambda_R/FWHM \times S = QF \times S \quad (8)$$

Figures 1–4 show *Q*(*sca*) (scattering efficiency), *Q*(*abs*) (absorption efficiency), and *Q*(*ext*) (extinction efficiency) verus λ, resonance wavelength for PS/P4VP (50:50) and PS/P4VP (75:25) at the thickness of 50, 95, and 50, 150 nm, respectively, for the various values of refractive indices. It is clear from all the figures that the nature of the graphs remains the same, irrespective of refractive indices. Further, as shown in **Figures 1** and **2,** scattering efficiency initially increases with an increase in resonance wavelength; thereafter, it continuously decreases, ranging from 400 to 1200 nm. It is evident from **Figures 1** and **2** that two peak resonance wavelengths are found for PS/P4VP (50:50) at the thickness of 50 nm, whereas three peak wavelengths are found for PS/P4VP (50:50) at the thickness of 95 nm for all the values of refractive indices. The additional peak wavelength can be attributed to an increase in the size of the nanoparticle from an average of 80 nm to 95.4 nm. In the case of the absorption efficiencies, the nature of the graph is the same except the first peak appears to have vanished for all the refractive index measurements in PS/P4VP (50:50) at 95 nm, whereas two clear peaks appear in PS/P4VP (50:50) at 50 nm. The graphs of the absorption efficiencies do not register sharp peaks, as is clear from **Figures 1** and **2**. A peak near 400 nm in PS/P4VP (50:50) at the thickness

of 95 nm seems to advance and disappear towards a higher wavelength, but in PS/P4VP (50:50) at the thickness of 50 nm, a not-so-sharp peak appears. Similar trends have been found in PS/P4VP (75:25) for 50 and 150 nm (**Figures 3** and **4),** except for the for the sharp and clear peaks visible in PS/P4VP (75:25) for 150 nm in scattering, absorption, and extinction efficiencies. The optimum results have been found in PS/P4VP (75:25) for 150 nm, as evident from the graph and comparative glance in **Tables 1–4**. In the case of all the efficiencies, the peak resonance wavelength shifts towards a higher wavelength in all the samples for all the values of refractive indices.

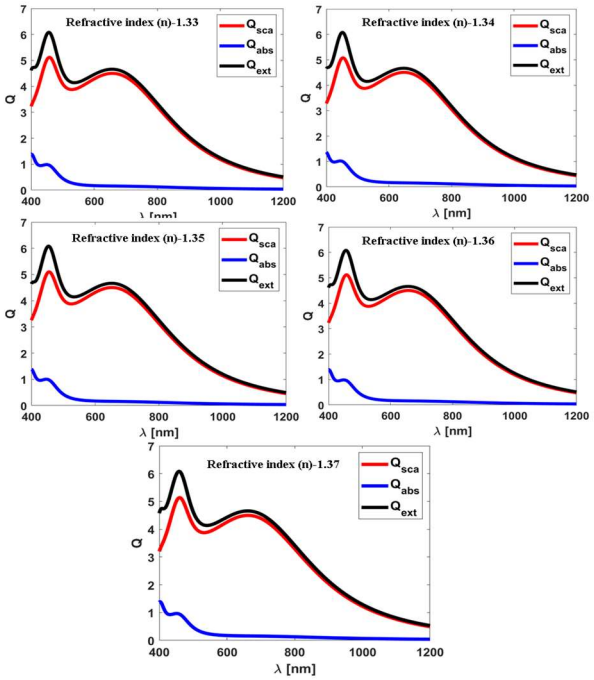

Figure 1. Plots of *Q*(*sca*), *Q*(*abs*) and *Q*(*ext*) vs. wavelength for different refractive index (*n*) for PS/P4VP 50:50 at 50 nm.

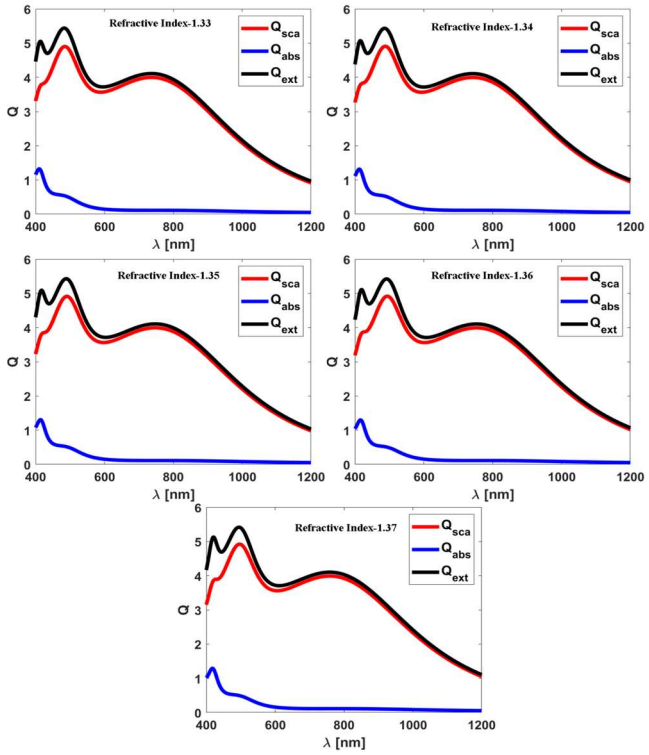

Figure 2. Plots of *Q*(*sca*), *Q*(*abs*) and *Q*(*ext*) vs. wavelength at various refractive index (*n*) for PS/P4VP 50:50 for film thickness 95 nm.

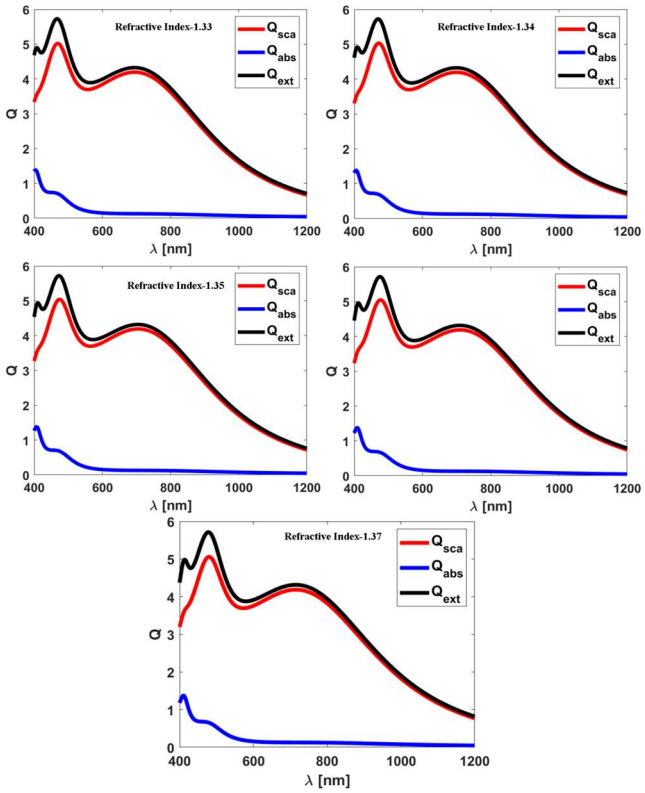

Figure 3. Plots of *Q*(*sca*), *Q*(*abs*) and *Q*(*ext*) vs. wavelength for PS/P4VP 70/25 for 50 nm.

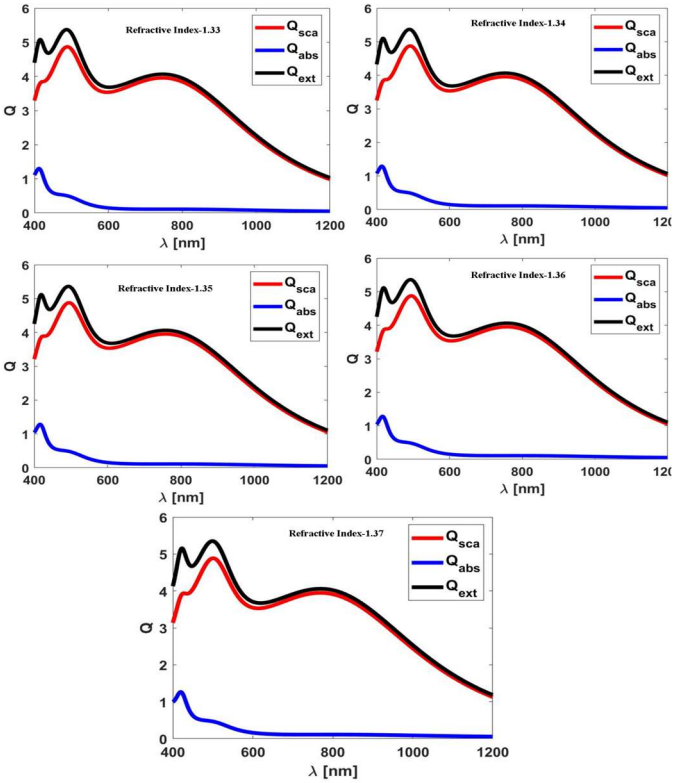

Figure 4. Plots of *Q*(*sca*), *Q*(*abs*) and *Q*(*ext*) vs. wavelength for PS/P4VP 70/25 for 150 nm.

Tables 1–4 compile the calculated values of λ_R, Q(sca), FWHM, QF, S, and FOM for all the samples at different values of refractive index, *n*. This database could be useful for selecting particular optical sensors with the requisite peak resonance wavelength. The resonance wavelength, λ_R is measured from the graph originally obtained by nano sensor software. It is evident that it is the size of the silver cluster that is responsible

for sensing the medium than the embedding polymer composite matrix. Hence, the results of PS/P4VP (50:50) at the thickness of 95 nm and PS/P4VP (75:25) at the thickness of 150 nm are almost the same. But the optimum result of PS/P4VP (75:25) for a thickness of 150 nm is economically viable.

Table 1. The comparison of sensing performance parameters for PS: P4VP/50:50 (organized with the thickness of 50 nm of silver particulate film). The system is considered to be embedded with silver clusters in the polymer composite. Diameter of nanoparticle on an average 80 nm in the sensing medium, 1.33–1.37.

Parameters/sensing medium	1.33	1.34	1.35	1.36	1.37
λ_R (nm)	643.43	648.248	653.53	657.85	661.862
Q(sca)	5.057	5.078	5.098	5.117	5.135
FWHM (nm)	43.3	44.47	44.9	44.9	44.844
S (nm/RIU)	481.8	528.2	432	401.2	460.8
QF	14.86	14.577	14.54	14.651	14.759
FOM (nm/RIU)	7159.45898	7699.676	6287.861	5878.161	6801.044

Table 2. The comparison of sensing performance parameters for PS: P4VP/50:50 (organized with the thickness of 95 nm of silver). The system is considered to be embedded with silver clusters in the polymer composite. Diameter of nanoparticle on an average 95.4 nm in the sensing medium, 1.33–1.37.

Parameters/sensing medium	1.33	1.34	1.35	1.36	1.37
λ_R (nm)	736.366	741.942	747.548	753.153	758.759
Q(sca)	4.908	4.907	4.912	4.916	4.921
FWHM (nm)	49.6	50.4	51.2	51.2	52
S (nm/RIU)	557.6	560.6	560.5	560.6	559.825
QF	14.846	14.72	14.6	14.71	14.59
FOM (nm/RIU)	8278.17906	8252.633	8183.607	8246.437	8168.697

Table 3. The comparison of sensing performance parameters for PS: P4VP/75:25 (organized with the thickness of 50 nm of silver). The system is considered to be embedded with silver clusters in the polymer composite. Diameter of nanoparticle on an average 88.6 nm in the sensing medium, 1.33–1.37.

Parameters/sensing medium	1.33	1.34	1.35	1.36	1.37
λ_R (nm)	694.695	699.499	705.105	709.91	714.715
Q(sca)	5.019	5.029	5.039	5.049	5.058
FWHM (nm)	45.7	47.3	48.1	48	47.2
S (nm/RIU)	480.4	560.6	480.5	480.5	500.5
QF	15.201	14.788	14.659	14.733	15.142
FOM (nm/RIU)	7302.56	8290.153	7043.649	7079.207	7578.571

Table 4. The comparison of sensing performance parameters for PS: P4VP/75:25 (organized with the thickness of 150 nm of silver). The system is considered to be embedded with silver clusters in the polymer composite. Diameter of nanoparticle on an average 97 nm in the sensing medium, 1.33–1.37.

Parameters/sensing medium	1.33	1.34	1.35	1.36	1.37
λ_R (nm)	746.747	752.352	757.958	763.564	769.169
Q(sca)	4.868	4.872	4.876	4.88	4.883
FWHM (nm)	49.4	51.2	52	51.2	52.8
S (nm/RIU)	560.5	560.6	560.6	560.5	560.55
QF	15.116	14.694	14.576	14.913	14.567
FOM (nm/RIU)	8472.70635	8237.667	8171.37	8358.938	8165.865

Figure 5 shows the variation of the peak resonance wavelength. λ_R versus sensing medium, n for all the chosen samples. It can be seen from the graph that the value of λ_R is higher in the case of PS/P4VP (50:50) at a thickness of 95 nm and PS/P4VP (75:25) at a thickness of 150 nm. In both polymer composites, the size of the nanocluster is almost the same, i.e., 95.4 nm and 97 nm. Indeed, it is evident that the size of nanoparticles is important, irrespective of the polymer composition of the matrix. It has been found that λ_R increases with an increase in the refractive index of the sensing medium in the entire sample.

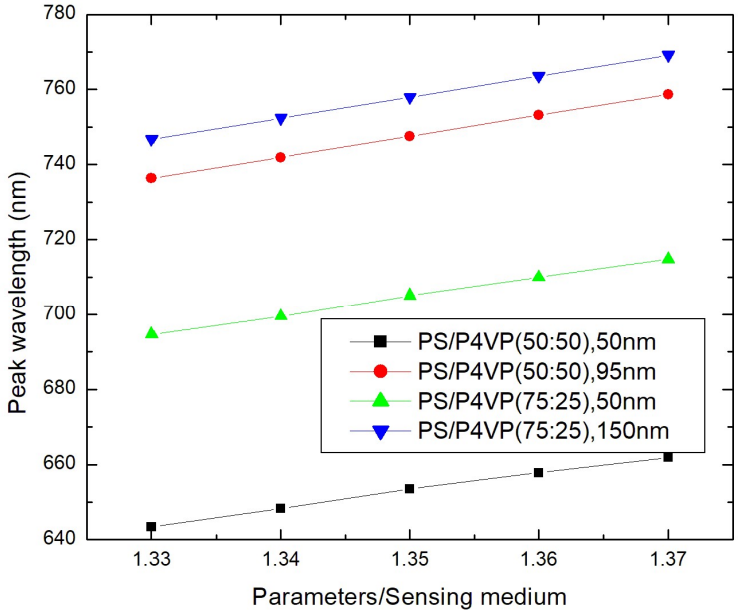

Figure 5. Sensing media vs. peak wavelength.

Figure 6 displays the scattering efficiency of a polymer composite embedded with silver nanoparticles versus a sensing medium. It is quite clear that the size of the silver cluster is a decisive factor for the scattering efficiency of the sample. The size of nanoparticles embedded in PS/P4VP (75:25) for 150 nm thickness is the maximum, hence the scattering efficiency is the lowest. The average size of nanoparticles is minimum in PS/P4VP (50:50) for 50 nm thickness; therefore, scattering efficiency is the highest. However, the efficiency of all the samples increases with the increase in sensing medium, *n*.

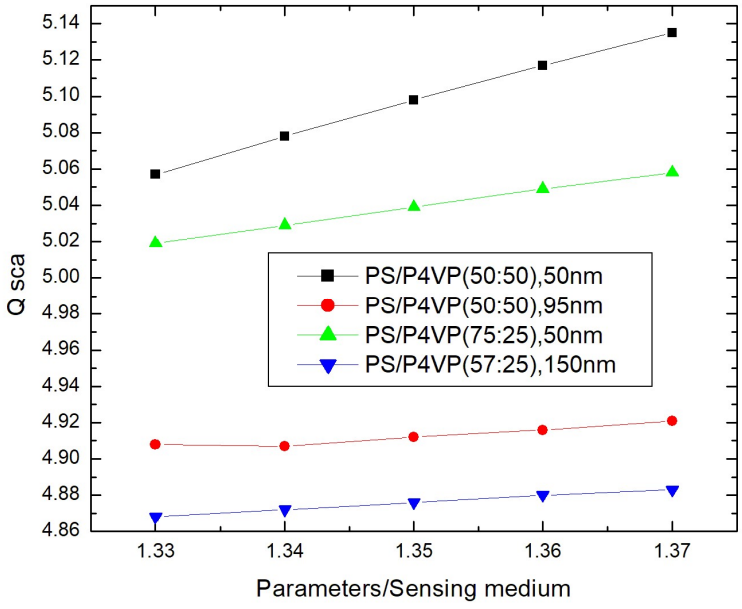

Figure 6. Sensing media vs. Q(sca).

The full width at half maximum (FWHM) of the resonant peak is plotted against the sensing medium, *n,* in **Figure 7**. This clearly shows that FWHM for all the samples increases with the increasing value of the sensing medium. It is highest for PS/P4VP (75:25), 150 nm, and lowest for PS/P4VP (50:50), 50 nm.

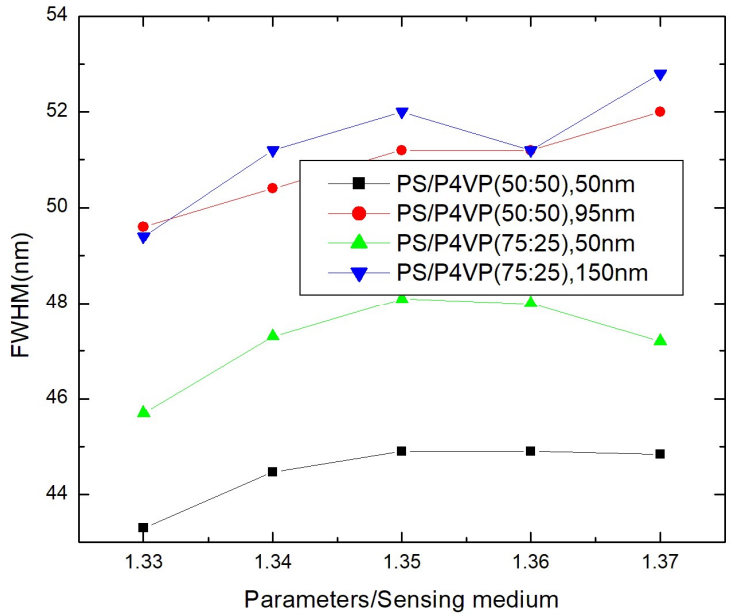

Figure 7. FWHM vs. sensitivity, M.

Figure 8 shows the variation of sensitivity, *S* versus sensing medium, for all the samples. It is visible that sensitivity is almost constant for PS/P4VP (75:25) at 150 nm and PS/P4VP (50:50) at 95 nm. For the rest of the two samples, *S* is variable with the sensing medium.

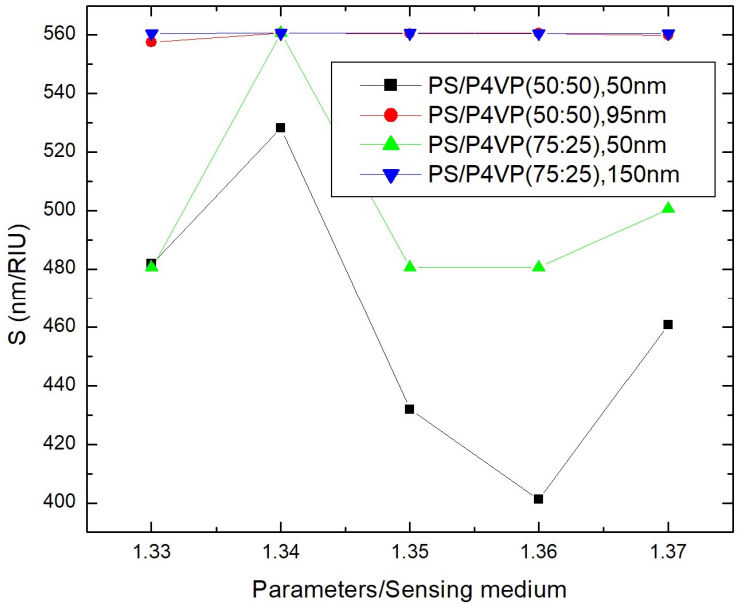

Figure 8. S nm-RIU vs. SM.

The quality factor versus sensing medium is shown in **Figure 9** for all the samples. QF initially decreases to a minimum; thereafter, it increases with the sensing medium. QF of PS/P4VP (75:25) for both the thicknesses 50 and 150 nm is found to be on the better side than QF of PS/P4VP (50:50) for both the thicknesses 50 and 95 nm.

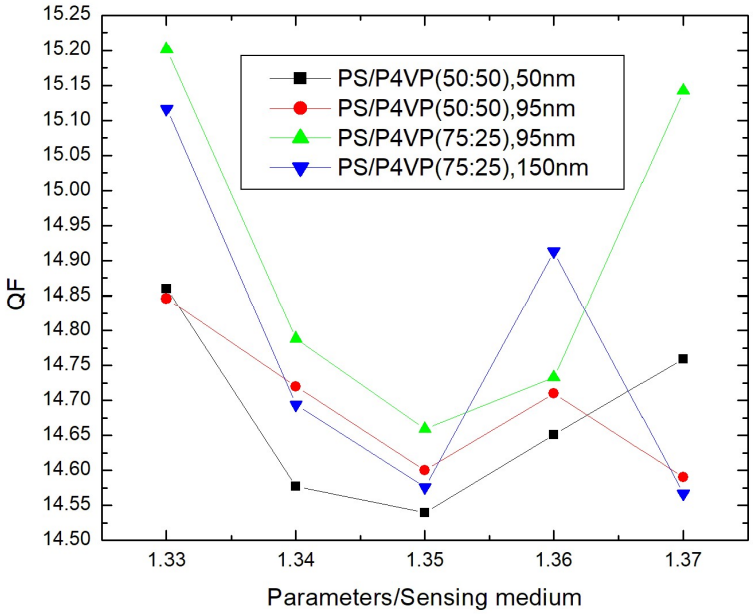

Figure 9. QF vs. SM.

4. Conclusions

The optical sensor properties of silver nanopolymer composites based on refractive index measurements have yielded good results. These silver nanocomposites were prepared by vapor deposition of silver on softened polymer composites kept in a vacuum of the order of 10^{-6} Torr. The previous studies have provided the optimum silver nanocomposites where silver nanoparticles are uniformly dispersed and almost the same size. The sensing properties seem to be dependent on the size distribution and dispersion of AgNP in polymer matrices. Therefore, the samples used here are expected to have better sensing properties. The database for the sensing parameters is computed in a table for future use. Also, these samples are prepared in thin film forms, so they are good for real-time application. The optical sensor results are found to be optimal in the polymer composite PS/P4VP (75:25) for 150 nm-thickness film. In the case of all the efficiencies, the peak resonance wavelength shifts towards a higher wavelength in all the samples for all the values of refractive indices. **Tables 1–4** provide a database for particular applications of nanosilver polymer composites.

Funding

This research received no external funding.

Acknowledgments

The author is grateful to department of applied physics, Gautam buddha university, Uttar Pradesh for providing the nano sensors lab software and providing help for execution of the same.

Conflict of interest

The author declares no conflict of interest.

Research data policy and data availability statements

All data generated or analyzed during this study are included in this published article [and its supplementary information files].

References

1. Wang G, Wang W, Wu J, et al. Self-assembly of a silver nanoparticles modified electrode and its electrocatalysis on neutral red. *Microchimica Acta* 2009; 164(1–2): 149–155.
2. Fang Q, Lafdi K. Development studies of silver nanocomposite based sensors for acid penetration. *Materials Today Proceedings* 2022; 52(2): 212–221. doi: 10.1016/j.matpr.2021.10.214
3. Melnikov P, Bobrov A, Marfin Y. On the use of polymer-based composites for the creation of optical sensors: A review. *Polymers* 2022; 14(20): 4448. doi: 10.3390/polym14204448
4. Cuppoletti J. *Metal, Ceramic and Polymeric Composites for Various Uses*. Intechopen; 2011.
5. Kyomuhimbo HD, Feleni U. Electroconductive green metal-polyaniline nanocomposites: Synthesis and application in sensors. *Electroanalysis* 2022; 35(2): e202100636. doi: 10.1002/elan.202100636
6. Kyomuhimbo HD, Michira IN, Mwaura FB, et al. Silver-zinc oxide nanocomposite antiseptic extract of bidens pilosa. *SN Applied Sciences* 2019; 681: 1. doi: 10.1007/s42452-019-0722-y
7. Paulraj P, Umar A, Rajendran K, et al. Solid-state synthesis of Ag-doped PANI nanocomposites for their end-use as an electrochemical sensor for hydrogen peroxide and dopamine. *Electrochimica Acta* 2020; 363: 137158. doi: 10.1016/j.electacta.2020.137158
8. Parashar P, Pattabi M, Gurumurthy SC. Electrical behaviour of discontinuous silver films deposited on softened polystyrene and poly (4-vinylpyridine) blends. *Journal of Materials Science: Materials in Electronics* 2009; 20: 1182–1185. doi: 10.1007/s10854-008-9848-1
9. Parashar P. Morphology of silver particulate films deposited on softened polymer blends of polystyrene and poly (4-vinylpyridine). *Journal of Applied Polymer Science* 2011; 121(2): 839–845. doi: 10.1002/app.33590
10. Parashar P. Electrical behaviour of discontinuous silver films deposited on compatible Polystyrene/Poly (2-vinylpyridine) composite. *Journal of Materials Science: Materials in Electronics* 2012; 23: 468–473. doi: 10.1007/s10854-011-0418-6
11. Bhadra J, Popelka A, Abdulkareem A, et al. Effect of humidity on the electrical properties of the silver-polyaniline/polyvinyl alcohol nanocomposites. *Sensonrs Actuators A: Physical* 2019; 288: 47–54. doi: 10.1016/j.sna.2019.01.012
12. Wang Y, Li Y, Yang S, et al. A convenient route to polyvinyl pyrrolidone/silver nanocomposite by electrospinning. *Nanotechnology* 2006; 17(13): 3304. doi: 10.1088/0957-4484/17/13/037
13. Bronstein LM, Sidorov SN, Valetsky PM. Nanostructured polymeric systems as nanoreactors for nanoparticle formation. *Russian Chemical Reviews* 2004; 73(5): 501–515. doi: 10.1070/RC2004v073n05ABEH000782
14. Wang X, Zuo J, Keil P, Grundmeier G. Comparing the growth of PVD silver nanoparticles on ultra thin fluorocarbon plasma polymer films and self-assembled fluoroalkyl silane monolayers. *Nanotecnology* 2007; 18(26): 265303. doi: 10.1088/0957-4484/18/26/265303
15. Kunz MS, Shull KR, Kellock AJ. Morphologies of discontinuous gold films on amorphous polymer substrates. *Journal of Applied Physics* 1992; 72: 4458–4460. doi: 10.1063/1.352362
16. Rao KM, Pattabi M, Sainkar SR, et al. Preparation and characterization of silver particulate structure deposited on softened poly (4-vinylpyridine) substrate. *Journal of Physics D: Applied Physics* 1999; 32(18): 2327. doi: 10.1088/0022-3727/32/18/303
17. Rao KM, Pattabi M. Effect of polymer-metal particle interaction on the structure of particulate silver films formed on softened polymer substrates. *Journal New Materials Electrochemical Systems* 2001; 4(1): 11–15.
18. Hassell T, Yoda S, Howdle SM, Brown PD. Microstructural characterization of silver/polymer nanocomposites prepared using supercritical carbon dioxide. *Journal of Physics: Conference Series* 2006; 26(1): 276–279. doi: 10.1088/1742-6596/26/1/066
19. Li X, Lenhart JJ, Walker HW. Dissolution-accompanied aggregation kinetics of silver nanoparticles. *Langmuir* 2010; 26(22): 16690–16698. doi: 10.1021/la101768n
20. Badawy AME, Luxton TP, Silva RG, et al. Impact of environmental conditions (pH, ionic strength, and electrolyte type) on the surface charge and aggregation of silver nanoparticles suspensions. *Environmental Science & Technology* 2010; 44(4): 1260–1266. doi: 10.1021/es902240k
21. Hotze EM, Phenrat T, Lowry GV. Nanoparticle aggregation: Challenges to understanding transport and reactivity in the environment. *Journal of Environmental Quality* 2010; 39(6): 1909–1924. doi: 10.2134/jeq2009.0462
22. Badawy AME, Luxton TP, Silva RG, et al. Impact of environmental conditions (pH, ionic strength, and electrolyte type) on the surface charge and aggregation of silver nanoparticles suspensions. *Environmental Science Technology* 2010; 44(4): 1260–1266. doi: 10.1021/es902240k
23. Loiseau A, Asila V, Aullen GB, et al. Silver-based plasmonic nanoparticles for and their use in biosensing. *Biosensors* 2019; 9(2): 78. doi: 10.3390/bios9020078
24. Tricoli A, Nasiri N, De S. Wearable and miniaturized sensor technologies for personalized and preventive medicine. *Advanced Functional Materials* 2017; 27(15): 1605271. doi: 10.1002/adfm.201605271
25. Zor SD, Cankurtaran H. Impedimetric humidity sensor based on nanohybrid composite of conducting poly (diphenylamine sulfonic acid). *Journal of Sensor* 2016; 2016(3): 1–9. doi: 10.1155/2016/5479092
26. Power AC, Betts AJ, Cassidy J. Silver nanoparticle polymer composite based humidity sensor. *The Analyst* 2010;

135(7): 1645–1652. doi: 10.1039/c0an00133c
27. Pathania P, Shishodia MS. Fano resonance-based blood plasma monitoring and sensing using plasmonic nanomatryoshka. *Plasmonics* 2021; 16: 2117–2124. doi: 10.1007/s11468-020-01343-z
28. Rajput P, Shishodia MS. Förster resonance energy transfer and molecular fluorescence near gain assisted refractory nitrides based plasmonic core-shell nanoparticle. *Plasmonics* 2020; 15: 2081–2093. doi: 10.1007/s11468-020-01208-5